

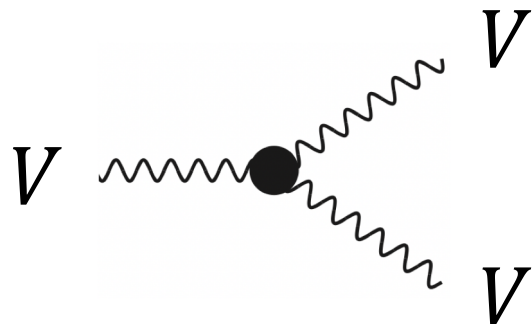
Mitchell Conference May 16 - 19, 2023

Anomalous triple gauge couplings in EW dilepton tails at the LHC and interference resurrection

Minho SON
KAIST

Hwang, Min, Park, **SON**, Yoo arXiv:2301.13663

anomalous Triple Gauge Coupling (aTGC)



$$\begin{aligned}
 \mathcal{L}_{TGC} = & ie \left[(W_{\mu\nu}^+ W_\mu^- - W_{\mu\nu}^- W_\mu^+) A_\nu + (1 + \delta\kappa_\gamma) A_{\mu\nu} W_\mu^+ W_\nu^- \right] \\
 & + ig_L \cos\theta \left[(1 + \delta g_{1,z}) (W_{\mu\nu}^+ W_\mu^- - W_{\mu\nu}^- W_\mu^+) Z_\nu + (1 + \delta\kappa_z) Z_{\mu\nu} W_\mu^+ W_\nu^- \right] \\
 & + ie \frac{\lambda_\gamma}{m_W^2} W_{\mu\nu}^+ W_{\nu\rho}^- A_{\rho\mu} + ig_L \cos\theta \frac{\lambda_z}{m_W^2} W_{\mu\nu}^+ W_{\nu\rho}^- Z_{\rho\mu}
 \end{aligned}$$

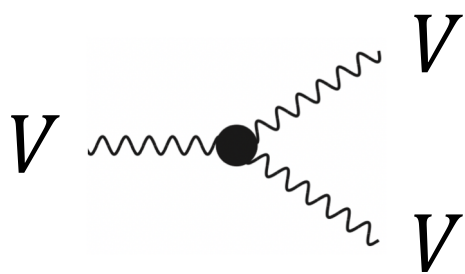
$$\delta\kappa_z = \delta g_{1,z} - \frac{g_Y^2}{g_L^2} \delta\kappa_\gamma \quad \lambda_z = \lambda_\gamma \quad \text{At the level of dim6 operators in SMEFT}$$

→ Three variables for VV

$$\underline{\{\lambda_z, \delta g_{1,z}, \delta\kappa_\gamma\}} \sim c^{(6)} \frac{m_W^2}{\Lambda^2}$$

We will mainly focus on this term in this talk

In terms of dim-6 operators



$$\lambda_z = \lambda_\gamma = c_{WWW} \frac{3g^2 m_W^2}{2\Lambda^2}$$

$$\text{tr}(W^3)$$

$$\delta\kappa_\gamma = (c_W + c_B) \frac{m_W^2}{2\Lambda^2}$$

$$\delta g_{1,z} = c_W \frac{m_Z^2}{2\Lambda^2}$$

CMS $Z(\ell\ell) + 2j$

Hagiwara et. al. (HISZ basis)

CMS $W\gamma$

Warsaw basis

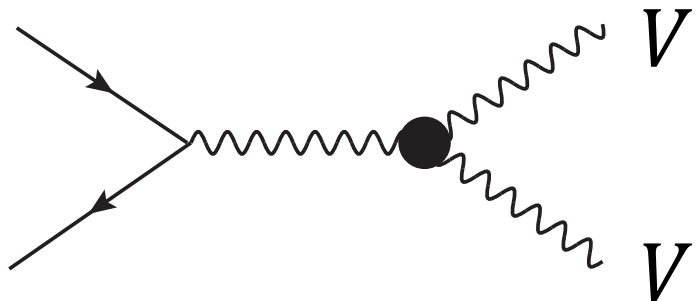
$$\frac{c_{WWW}}{\Lambda^2} \text{Tr}(\hat{W}_{\mu\nu} \hat{W}_{\nu\rho} \hat{W}_{\rho\mu})$$

$$C_{3W} \epsilon_{abc} W_{\mu\nu}^a W_{\nu\rho}^b W_{\rho\mu}^c$$

$$\frac{c_W}{\Lambda^2} (D_\mu H)^+ W^{a\,\mu\nu} \frac{\sigma^a}{2} g(D_\nu H)$$

$$\frac{c_B}{\Lambda^2} (D_\mu H)^+ B^{\mu\nu} \frac{1}{2} g'(D_\nu H)$$

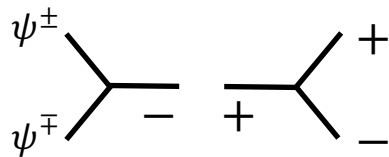
aTGC in VV process and noninterference



Helicity selection rule: total helicity should match

$$|h(A_3^{SM})| = 1 - [g] = 1$$

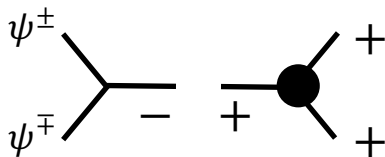
$$|h(A_3^{BSM})| = 1 - [c_{3W}] = 3$$



SM amplitude

Similarly for t-channel diagram

$$h(A_4^{SM}) = 0$$



**BSM amplitude
with insertion of $\mathcal{O}_{3W} \sim \text{tr}(W^3)$**

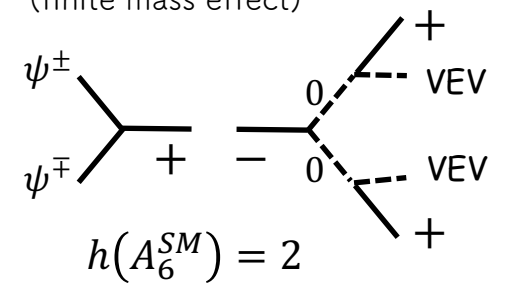
$$h(A_4^{BSM}) = 2$$



can not interfere in massless limit

Azatov, Contino, Machado, Riva 16'

Flip the helicity via VEV insertion
(finite mass effect)

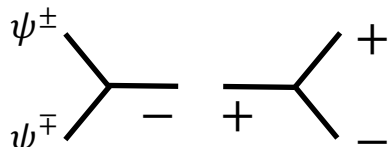


$$h(A_6^{SM}) = 2$$

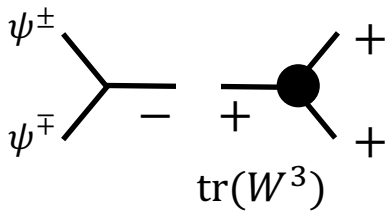
$$\propto \left(\frac{m_W}{E}\right)^2 = \varepsilon_V^2$$

Noninterference in VV process

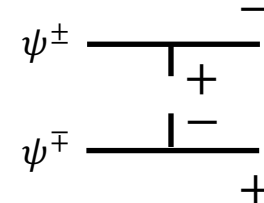
Helicity selection rule: total helicity should match



$$h(A_4^{SM}) = 0$$

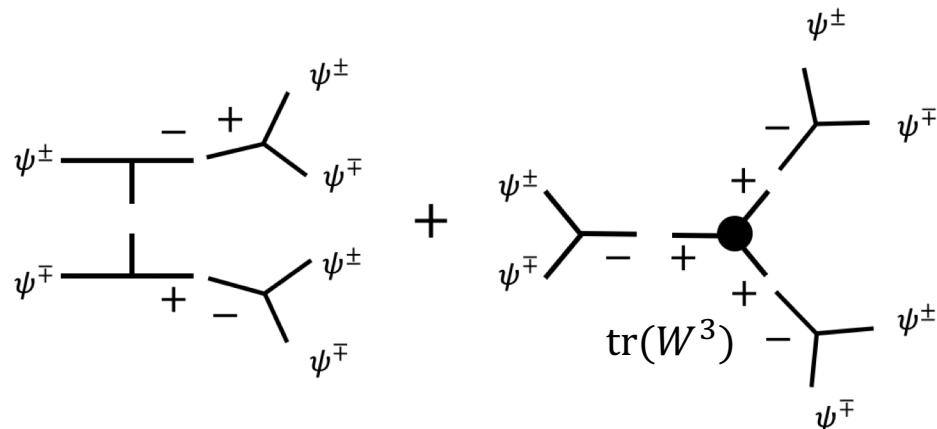


$$h(A_4^{BSM}) = 2$$



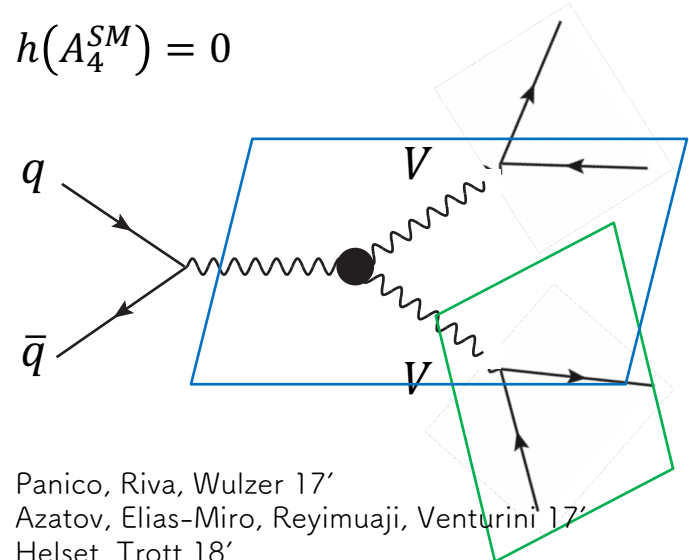
$$h(A_4^{BSM}) = 0$$

The correct picture is that, in fact, they do interfere in a full amplitude



$$\int d\phi \frac{(\mathcal{M}_{SM}^* \mathcal{M}_{BSM} + h.c.)}{\neq 0}$$

: suggests us to look into differential distributions of angular variable



Panico, Riva, Wulzer 17'

Azatov, Elias-Miro, Reyimuaji, Venturini 17'

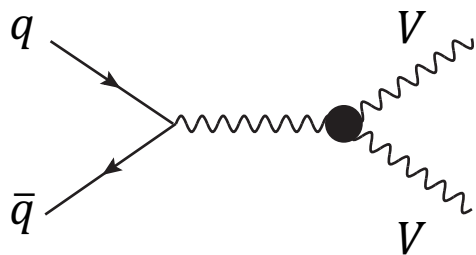
Helset, Trott 18'

Aoude, Shepherd 19'

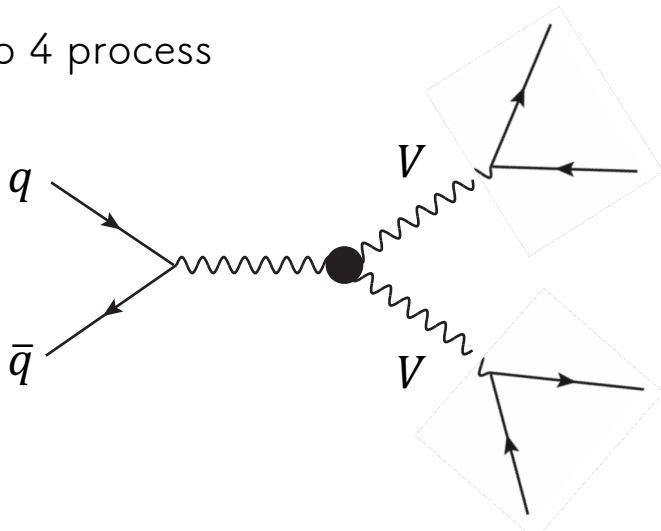
+ ...

Noninterference in VV process

2 to 2 process, subject to non-interference



2 to 4 process



SMxdim6 scales like

$$\sim \sigma_{SM} \frac{E^2}{\Lambda^2} \times \left(\frac{m_W}{E} \right)^2 \sim \frac{m_W^2}{\Lambda^2}$$

dim6xdim6 scales like

$$\sim \sigma_{SM} \frac{E^4}{\Lambda^4}$$

$$\sigma = \sigma^{SM} + \sum \left(\frac{c_i^{(6)}}{\Lambda^2} \sigma_i^{(6 \times SM)} + h.c. \right) + \sum \frac{c_i^{(6)} c_j^{(6)*}}{\Lambda^4} \sigma_{ij}^{(6 \times 6)} + \dots$$

- $\Delta c^{(6)} \propto \sqrt{\Delta \sigma}$ (v.s. $\Delta c^{(6)} \propto \Delta \sigma$ in case interference)
- EFT expansion fails, e.g. SMxdim8 \sim dim6xdim6, what if SMxdim8 can interfere without suppression?

SMxdim8 appears not suppressed

Degrade and Li arXiv:2303.10493

Thus, from EFT point of view, naively, power counting goes like

$$\sim \frac{E^2}{\Lambda^2}$$

$$\sim \frac{E^4}{\Lambda^4}$$

$$\frac{d\sigma/d\phi}{d\sigma_{SM}/d\phi} = 1 + \sum \left(\frac{c_i^{(6)}}{\Lambda^2} \frac{d\sigma_i^{(6 \times SM)}}{d\sigma_{SM}/d\phi} / d\phi + h.c. \right) + \sum \frac{c_i^{(6)} c_j^{(6)*}}{\Lambda^4} \frac{d\sigma_{ij}^{(6 \times 6)}}{d\sigma_{SM}/d\phi} / d\phi + \dots$$

Resurrection of interference



CMS-SMP-20-005

CERN-EP-2021-219
2022/03/11

Measurement of $W^\pm\gamma$ differential cross sections in proton-proton collisions at $\sqrt{s} = 13$ TeV and effective field theory constraints

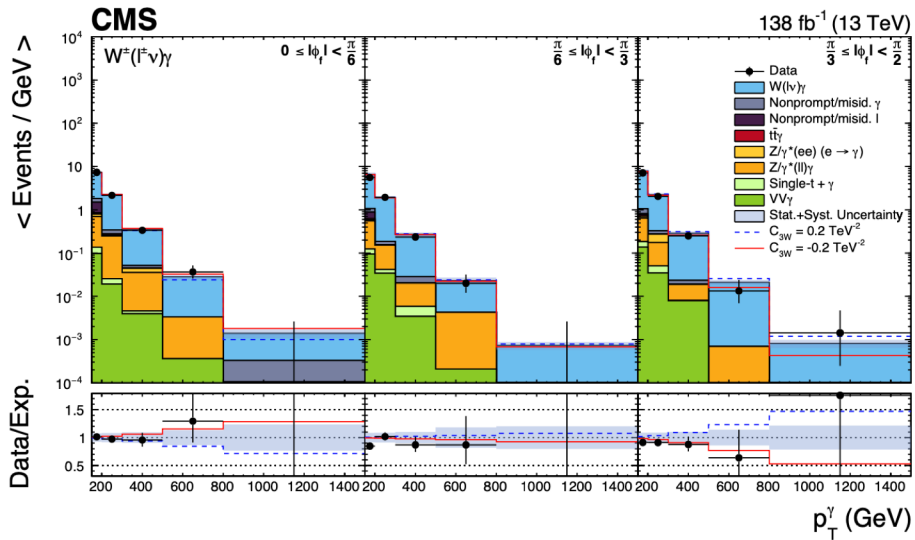
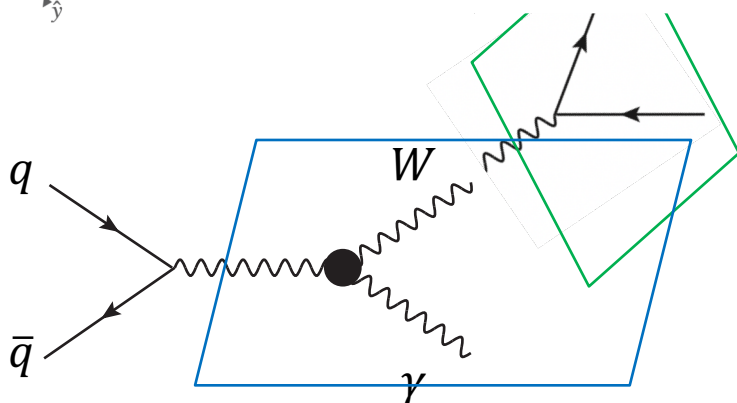
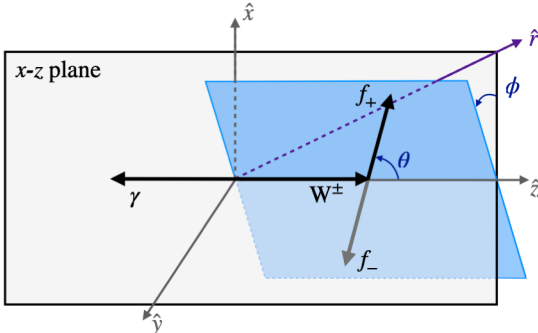


Table 4: Best fit values of C_{3W} and corresponding 95% CL confidence intervals as a function of the maximum p_T^γ bin included in the fit.

p_T^γ cutoff (GeV)	Best fit C_{3W} (TeV^{-2}) SM+int. only	Best fit C_{3W} (TeV^{-2}) SM+int.+BSM	Observed 95% CL (TeV^{-2}) SM+int. only	Observed 95% CL (TeV^{-2}) SM+int.+BSM	Expected 95% CL (TeV^{-2}) SM+int. only	Expected 95% CL (TeV^{-2}) SM+int.+BSM
200	-0.86	-0.24	[-2.01, 0.38]	[-0.76, 0.40]	[-1.16, 1.27]	[-0.81, 0.71]
300	-0.25	-0.17	[-0.81, 0.34]	[-0.39, 0.28]	[-0.56, 0.60]	[-0.33, 0.33]
500	-0.13	-0.025	[-0.50, 0.25]	[-0.15, 0.12]	[-0.35, 0.38]	[-0.17, 0.16]
800	-0.20	-0.033	[-0.49, 0.11]	[-0.10, 0.08]	[-0.29, 0.31]	[-0.097, 0.095]
1500	-0.13	-0.009	[-0.38, 0.17]	[-0.062, 0.052]	[-0.27, 0.29]	[-0.066, 0.065]

$$C_{3W}\epsilon_{ijk}W_{\mu\nu}^iW_{\nu\rho}^jW_{\rho\mu}^k$$

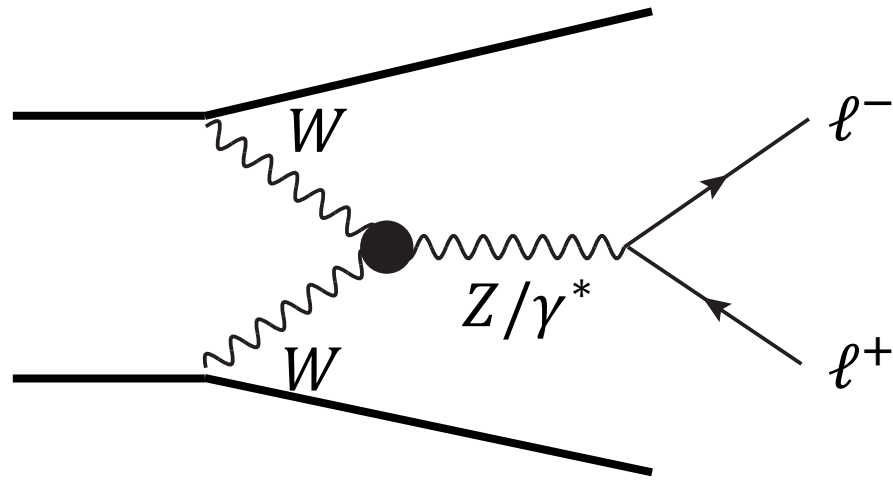
Observed 95% CL (TeV^{-2}) SM+int. only	Observed 95% CL (TeV^{-2}) SM+int.+BSM
[-0.38, 0.17]	[-0.062, 0.052]

We newly add

2-to-4 dilepton + 2 jets

to the list as a new way of resurrecting interference

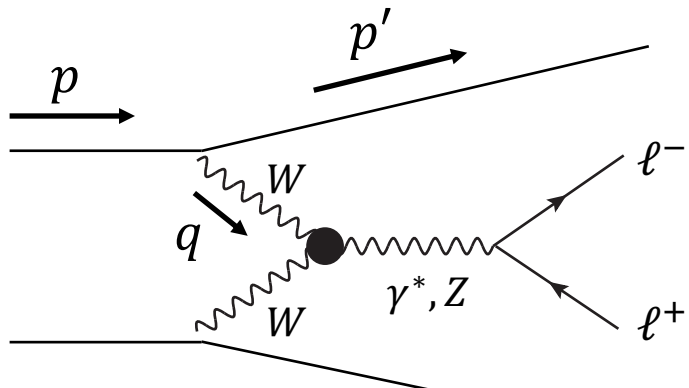
Hwang, Min, Park, SON, Yoo arXiv:2301.13663



Interference resurrection in the total cross section

Effective W Approximation (EWA)

: factorization. Total result \sim treating W as on-shell and convolute xsec with W PDF



$$V^2 \equiv m^2 - q^2$$

$$= m^2 - (p - p')^2$$

Time interval during which
virtual W can not be
distinguished from on-shell W

$$\Delta t \sim \frac{E}{V^2}$$

Interaction scale of
hard-process

$$t \sim \frac{1}{E}$$

V : Virtuality of W boson

E : Energy scale of hard-process

Relevant phase space for EWA

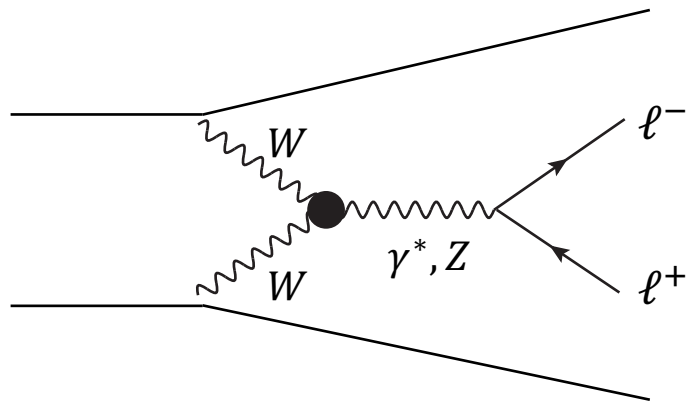
$$xE \sim (1-x)E, \quad \delta_m = \frac{m}{E} \ll 1, \quad \delta_\perp = \frac{p_T}{E} \ll 1 \quad \rightarrow \quad \Delta t \sim \frac{E}{V^2} \gg t \sim \frac{1}{E}$$

: factorization can be rigorously proven to work

$$\frac{d\sigma_{EWA}(q_i \bar{q}_j \rightarrow q'_i \bar{q}'_j X)}{dx_i dx_j dp_{\perp,i} dp_{\perp,j}} = \sum_{r,s} \frac{C_i^2}{2\pi^2} \frac{C_j^2}{2\pi^2} f_r(x_i, p_{\perp,i}) f_s(x_j, p_{\perp,j}) \times \boxed{d\sigma(W_r^{q_i} W_s^{q_j} \rightarrow X)}$$

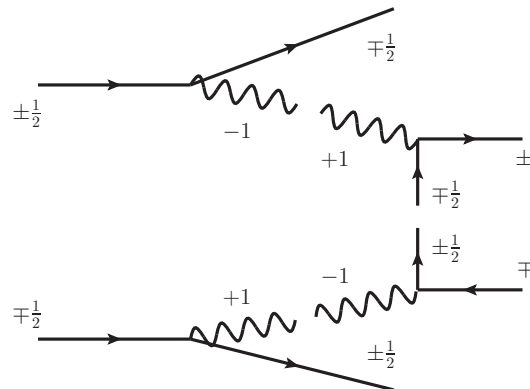
Apparent 2-to-2 process seems
to be subject to noninterference.

Interference resurrection



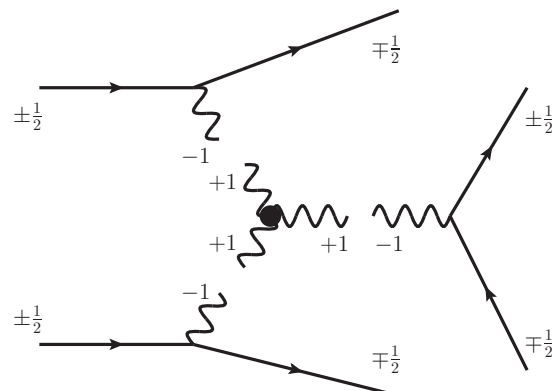
With quark currents attached to both vector bosons, interference seem to be recovered

SM diagram unsuppressed



Order-one effect from
t-channel type (enhanced
soft phase space) ?

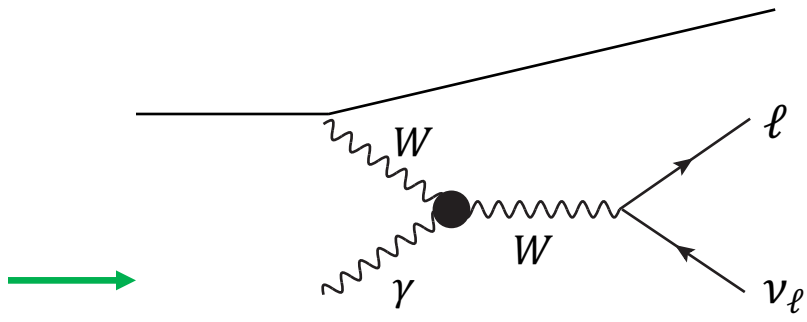
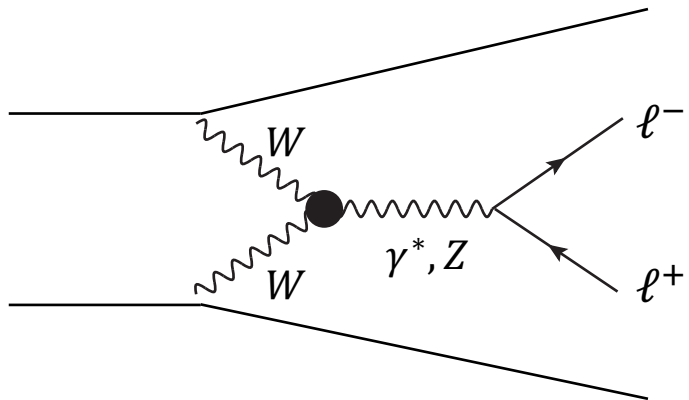
BSM diagram



Many radiation type diagrams

Analytic study of resurrection of interference with a toy process

: analytic calculation of 2-to-4 amplitude is extremely challenging, maybe impossible



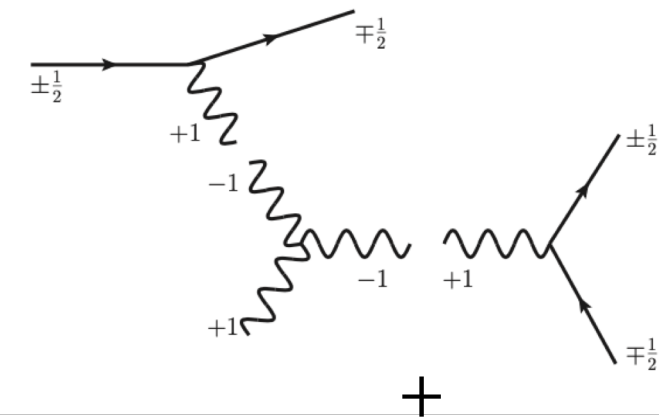
2-to-3 process is analytically calculable

Replace one W with γ for simplicity
→ only one type of the gauge boson

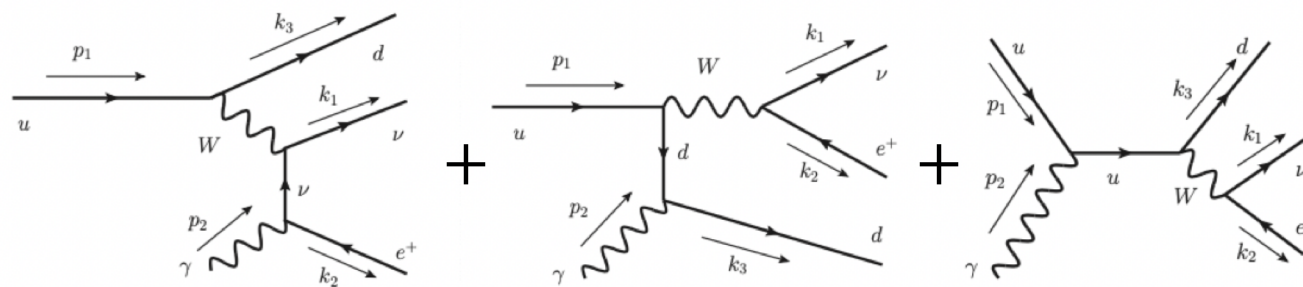
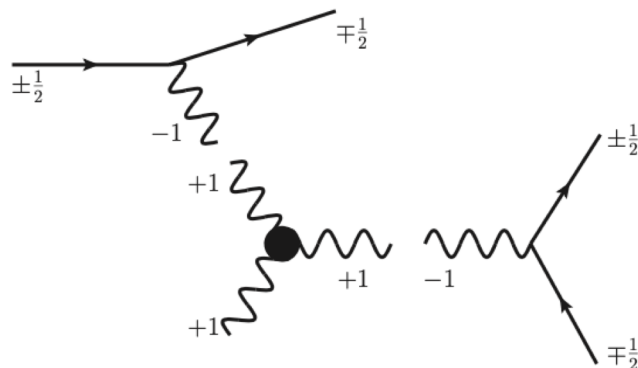
Calculable 2-to-3 toy example

: better to understand structure

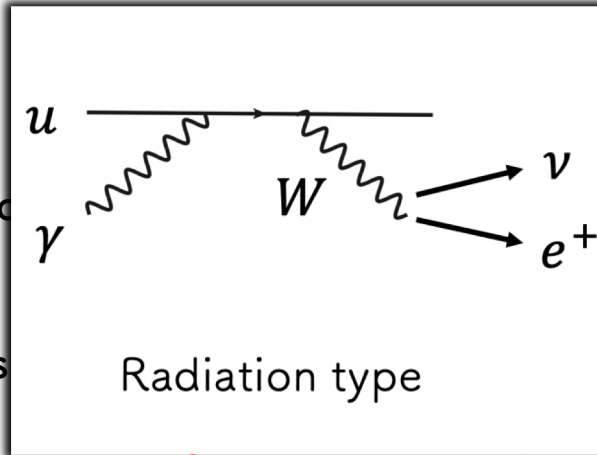
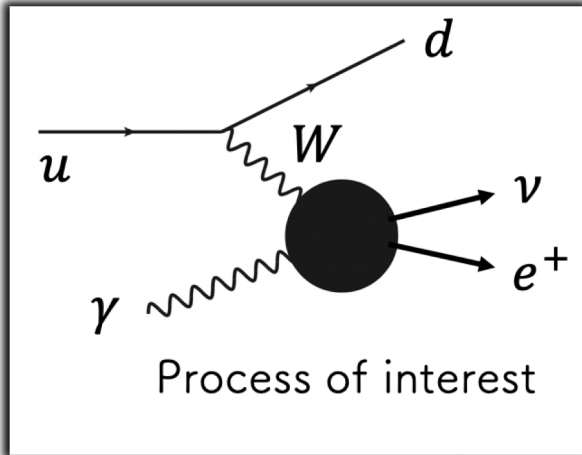
SM diagrams



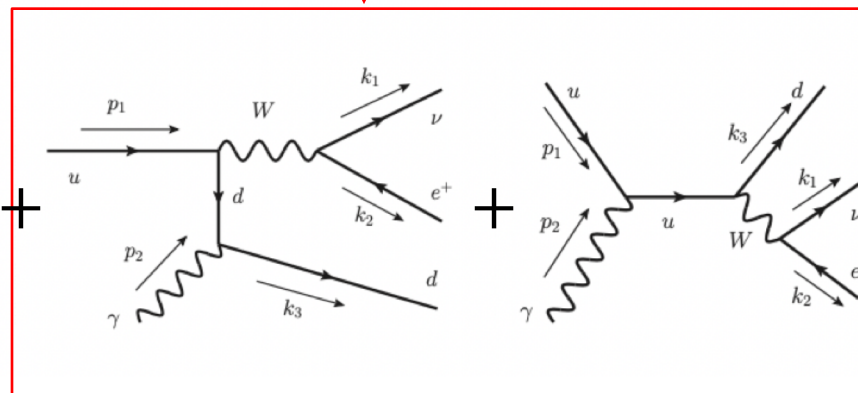
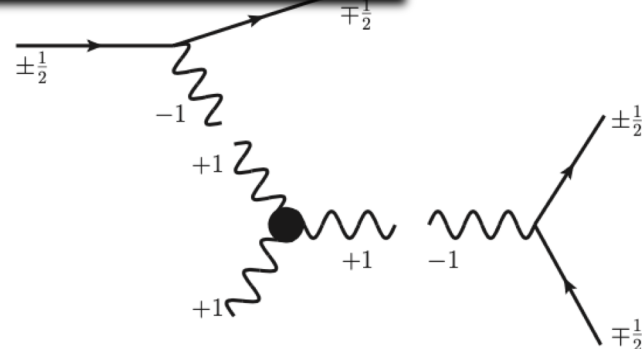
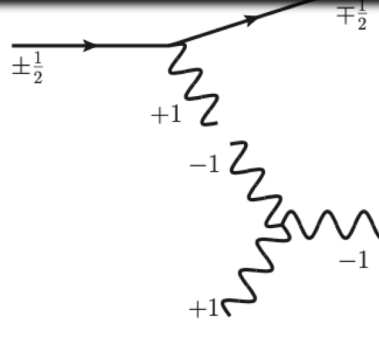
BSM diagrams



In the unitary gauge

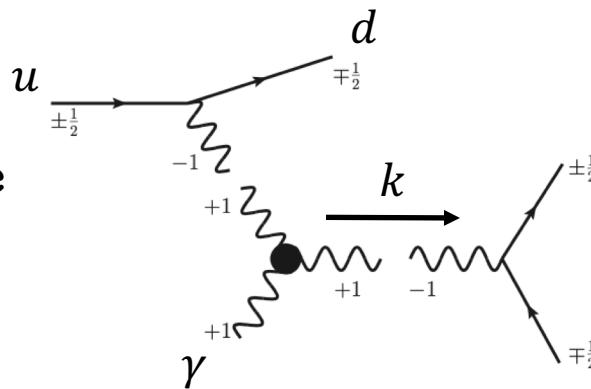


Diagrams



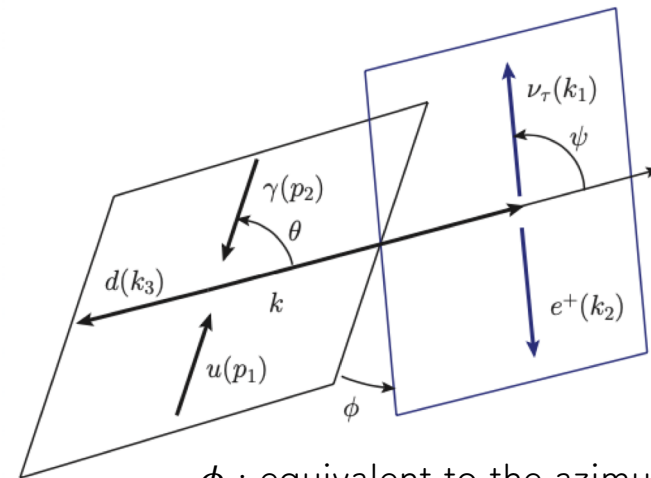
One can choose a gauge where these two diagrams are trashed, but they are important to get correct high E behavior and satisfy Ward identity in general.

Toy Example : 2-to-3



$$k^\mu = (z\sqrt{\hat{s}}, 0, 0, (1-z)\sqrt{\hat{s}})$$

z : fraction of energy flowing into $\ell\nu$ system



ϕ : equivalent to the azimuthal angle of the forward quark

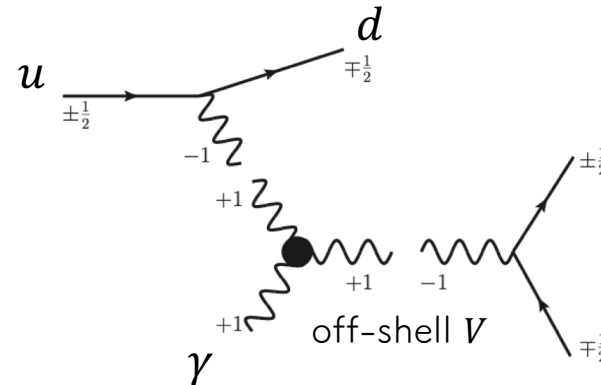
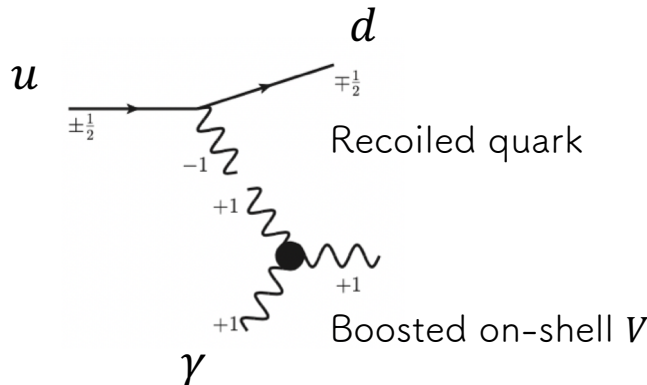
1. For W mass window

Narrow width approximation applied

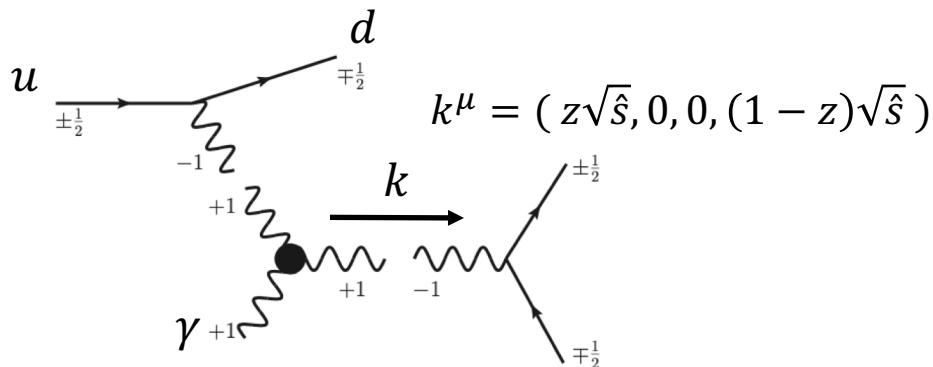
$$[k^2 = m_{\ell\nu}^2 = (2z - 1)\hat{s} \sim m_W^2]$$

2. Off-shell region away from mass window

$$[k^2 = m_{\ell\nu}^2 = (2z - 1)\hat{s} \gg m_W^2]$$



Toy Example : 2-to-3



1. For W mass window [$k^2 = m_{\ell\nu}^2 = (2z - 1)\hat{s} \sim m_W^2$]

Narrow width approximation applied

For $\hat{s} \gg m_W^2$

$$\frac{d\hat{\sigma}_{\text{SM}\times\text{BSM}}}{d\phi} \sim \frac{1}{4} \frac{\lambda_z}{512 \pi^4} \frac{\pi e^2 g^4}{3} \frac{2}{m_W \Gamma_W} \left[\cos(2\phi) \left(2 - \log \frac{\hat{s}}{m_W^2} \right) \right]$$

$$\frac{d\hat{\sigma}_{\text{BSM}^2}}{d\phi} \sim \frac{1}{4} \frac{\lambda_z^2}{512 \pi^4} \frac{\pi e^2 g^4}{6} \frac{\hat{s}}{m_W^3 \Gamma_W}$$

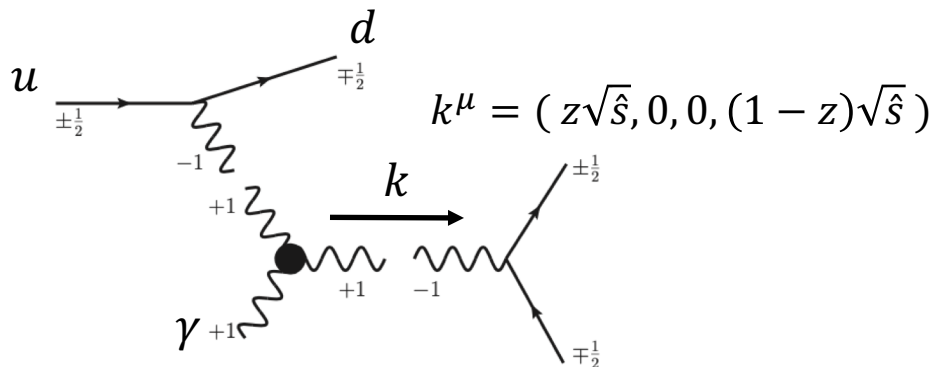
2. Off-shell region away from mass window [$k^2 = m_{\ell\nu}^2 = (2z - 1)\hat{s} \gg m_W^2$]

For $\hat{s} \gg m_W^2$

$$\frac{d\hat{\sigma}_{\text{SM}\times\text{BSM}}(u_L \gamma_L \rightarrow d v e^+)}{d\phi} \sim \frac{\lambda_z}{512 \pi^4} \frac{e^2 g^4}{m_W^2} \left[-\frac{2}{9} - \frac{\pi^2}{6} \cos\phi + \frac{1}{18} \left(\pi^2 - 26 + 22 \ln \frac{\hat{s}}{m_W^2} - 6 \ln^2 \frac{\hat{s}}{m_W^2} \right) \cos(2\phi) \right]$$

$$\frac{d\hat{\sigma}_{\text{BSM}^2}(u_L \gamma_L \rightarrow d v e^+)}{d\phi} \sim \frac{\lambda_z^2}{512 \pi^4} e^2 g^4 \frac{\hat{s}}{m_W^4} \left[\frac{1}{24} \left(-9 + 4 \ln \frac{\hat{s}}{m_W^2} \right) - \frac{\pi^2}{48} \cos\phi - \frac{1}{12} \cos(2\phi) \right]$$

Toy Example : 2-to-3



1. For W mass window [$k^2 = m_{\ell\nu}^2 = (2z - 1)\hat{s} \sim m_W^2$]

Narrow width approximation applied

For $\hat{s} \gg m_W^2$

$$\frac{d\hat{\sigma}_{\text{SM}\times\text{BSM}}}{d\phi} \sim \frac{1}{4} \frac{\lambda_z}{512 \pi^4} \frac{\pi e^2 g^4}{3} \frac{2}{m_W \Gamma_W} \left[\cos(2\phi) \left(2 - \log \frac{\hat{s}}{m_W^2} \right) \right]$$

Suppressed by a factor of $\sim \mathcal{O}\left(\frac{\Gamma_W}{m_W}\right) \times$

$$\frac{d\hat{\sigma}_{\text{BSM}^2}}{d\phi} \sim \frac{1}{4} \frac{\lambda_z^2}{512 \pi^4} \frac{\pi e^2 g^4}{6} \frac{\hat{s}}{m_W^3 \Gamma_W}$$

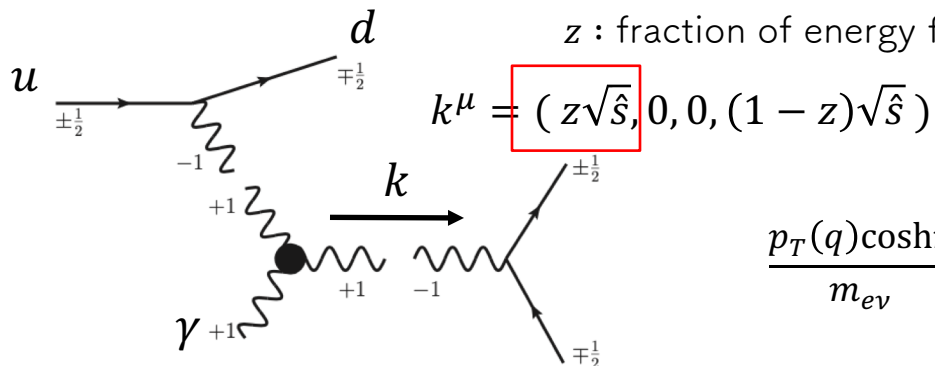
2. Off-shell region away from mass window [$k^2 = m_{\ell\nu}^2 = (2z - 1)\hat{s} \gg m_W^2$]

For $\hat{s} \gg m_W^2$

$$\frac{d\hat{\sigma}_{\text{SM}\times\text{BSM}}(u_L \gamma_L \rightarrow d v e^+)}{d\phi} \sim \frac{\lambda_z}{512 \pi^4} \frac{e^2 g^4}{m_W^2} \left[-\frac{2}{9} - \frac{\pi^2}{6} \cos\phi + \frac{1}{18} \left(\pi^2 - 26 + 22 \ln \frac{\hat{s}}{m_W^2} - 6 \ln^2 \frac{\hat{s}}{m_W^2} \right) \cos(2\phi) \right]$$

$$\frac{d\hat{\sigma}_{\text{BSM}^2}(u_L \gamma_L \rightarrow d v e^+)}{d\phi} \sim \frac{\lambda_z^2}{512 \pi^4} e^2 g^4 \frac{\hat{s}}{m_W^4} \left[\frac{1}{24} \left(-9 + 4 \ln \frac{\hat{s}}{m_W^2} \right) - \frac{\pi^2}{48} \cos\phi - \frac{1}{12} \cos(2\phi) \right]$$

Toy Example : 2-to-3



z : fraction of energy flowing into $\ell\nu$ system

1. For W mass window [$k^2 = m_{\ell\nu}^2 = (2z - 1)\hat{s} \sim m_W^2$]

Narrow width approximation applied

For $\hat{s} \gg m_W^2$

$$\frac{d\hat{\sigma}_{\text{SM}\times\text{BSM}}}{d\phi} \sim \frac{1}{4} \frac{\lambda_z}{512 \pi^4} \frac{\pi e^2 g^4}{3} \frac{2}{m_W \Gamma_W} \left[\cos(2\phi) \left(2 - \frac{1}{2} \right) + \sin(2\phi) \left(\frac{1}{2} \right) \right]$$

$$\frac{d\hat{\sigma}_{\text{BSM}^2}}{d\phi} \sim \frac{1}{4} \frac{\lambda_z^2}{512 \pi^4} \frac{\pi e^2 g^4}{6} \frac{\hat{s}}{m_W^3 \Gamma_W}$$

2. Off-shell region away from mass window

For $\hat{s} \gg m_W^2$

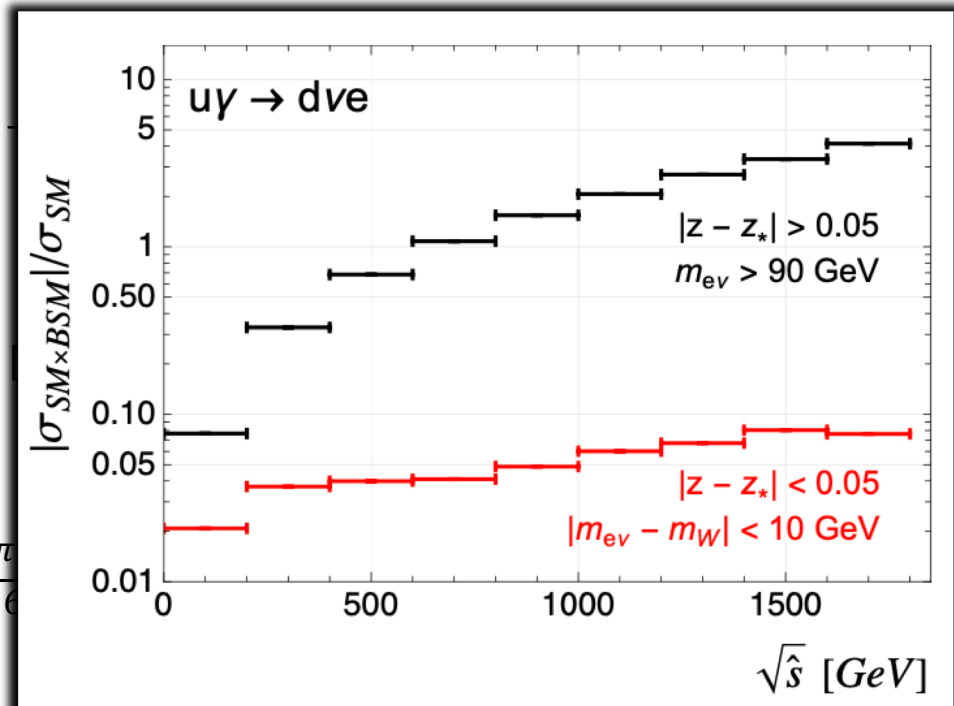
$$\frac{d\hat{\sigma}_{\text{SM}\times\text{BSM}}(u_L \gamma_L \rightarrow d v e^+)}{d\phi} \sim \frac{\lambda_z}{512 \pi^4} \frac{e^2 g^4}{m_W^2} \left[-\frac{2}{9} - \frac{\pi}{6} \tan(\phi) \right]$$

$$\frac{d\hat{\sigma}_{\text{BSM}^2}(u_L \gamma_L \rightarrow d v e^+)}{d\phi} \sim \frac{\lambda_z^2}{512 \pi^4} e^2 g^4 \frac{\hat{s}}{m_W^4} \left[\frac{1}{24} \left(-9 + 4 \ln \frac{\hat{s}}{m_W^2} \right) - \frac{48}{48} \cos\phi - \frac{12}{12} \cos(z\phi) \right]$$

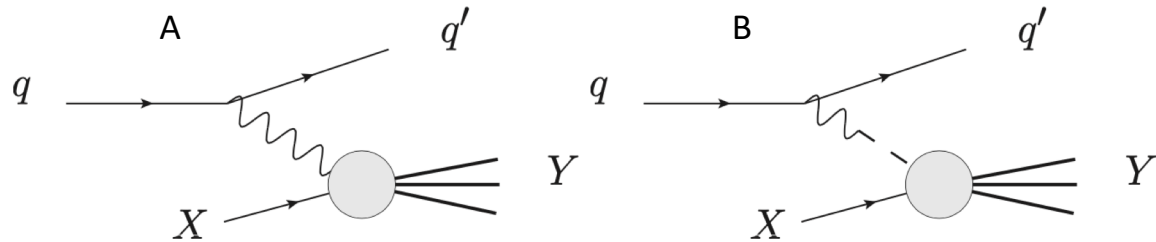
$$\frac{p_T(q) \cosh\eta}{m_{ev}} = \frac{1-z}{\sqrt{2z-1}} \leq \frac{1-z_{\min}}{\sqrt{2z_{\min}-1}} = \delta_{\min}$$

$$p_T(q) \leq \delta_{\min} \frac{m_{ev}}{\cosh\eta}$$

Numerical confirmation



Derivation of EWA : factorization



Derivation in the axial gauge

$$\mathcal{A}_{\text{total}}^{\text{sc-A}} = -\frac{i}{V^2} \sum_{h=\pm 1} \left[J^\mu (\varepsilon_\mu^h)^* \right] \left[\varepsilon_\nu^h \mathcal{A}_Q^\nu \right] - \frac{i}{V^2} \left[J^\mu (\varepsilon_\mu^0)^* \right] \left[\left(1 - \frac{V^2}{m^2} \right) \varepsilon_\nu^0 \mathcal{A}_Q^\nu \right] [1 + \mathcal{O}(\delta_\perp^2 + \delta_m^2)]$$

$$\delta_m = \frac{m}{E} \ll 1, \quad \delta_\perp = \frac{p_T}{E} \ll 1$$

$$-\frac{i}{V^2} \left[J^\mu (\varepsilon_\mu^\pm)^* \right] = 2C \frac{p_\perp e^{\pm i\phi}}{V^2} g_\pm(x) (1 + \mathcal{O}(\delta_\perp^2 + \delta_m^2))$$

$$g_\pm(x) \left[\varepsilon_\nu^\pm \mathcal{A}^\nu \right] = \mathcal{A}_\pm = \mathcal{A}_\pm^{(0,0)} + \mathcal{A}_\pm^{(1,0)} \frac{\tilde{p}_\perp}{E} + \mathcal{A}_\pm^{(0,1)} \frac{\tilde{p}_\perp^*}{E} + \dots$$

Including only transverse polarization ...

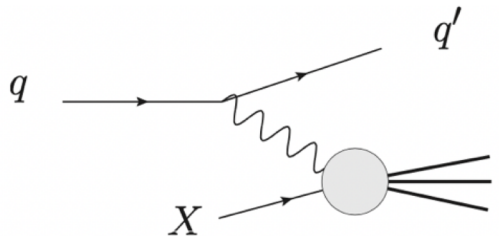
$$\mathcal{A}_{\text{total}} = \frac{2C}{V^2} [\tilde{p}_\perp \mathcal{A}_+ + \tilde{p}_\perp^* \mathcal{A}_-]$$

$$\tilde{p}_\perp \equiv p_1 - ip_2 = p_\perp e^{-i\phi}, \quad \tilde{p}_\perp = p_\perp e^{i\phi}$$

: azimuthal angle

$$\begin{aligned} &= \frac{2C}{V^2} \left[\tilde{p}_\perp \left(\mathcal{A}_+^{(0,0)} + \mathcal{A}_+^{(1,0)} \frac{\tilde{p}_\perp}{E} + \mathcal{A}_+^{(0,1)} \frac{\tilde{p}_\perp^*}{E} + \dots \right) \right. \\ &\quad \left. + \tilde{p}_\perp^* \left(\mathcal{A}_-^{(0,0)} + \mathcal{A}_-^{(1,0)} \frac{\tilde{p}_\perp}{E} + \mathcal{A}_-^{(0,1)} \frac{\tilde{p}_\perp^*}{E} + \dots \right) \right] \end{aligned}$$

Derivation of EWA : factorization



Including only transverse polarization ...

$$\mathcal{A}_{\text{total}} = \frac{2C}{V^2} \left[\tilde{p}_\perp \left(\mathcal{A}_+^{(0,0)} + \mathcal{A}_+^{(1,0)} \frac{\tilde{p}_\perp}{E} + \mathcal{A}_+^{(0,1)} \frac{\tilde{p}_\perp^*}{E} + \dots \right) + \tilde{p}_\perp^* \left(\mathcal{A}_-^{(0,0)} + \mathcal{A}_-^{(1,0)} \frac{\tilde{p}_\perp}{E} + \mathcal{A}_-^{(0,1)} \frac{\tilde{p}_\perp^*}{E} + \dots \right) \right]$$

$$\tilde{p}_\perp \equiv p_1 - ip_2 = p_\perp e^{-i\phi}, \tilde{p}_\perp^* = p_\perp e^{i\phi}$$

$$\begin{aligned} d\sigma(qX \rightarrow q'Y)_{\text{EWA}} &= \frac{1}{2E_q E_X |1 - v_X|} \int_{\phi} \frac{|\mathcal{A}^{(0,0)}|^2}{2} \frac{d^3 p_{q'}}{2E_{q'} (2\pi)^3} d\Phi_Y (2\pi)^4 \delta^4(p_Y + p_{q'} - p_q - p_X) \\ &\simeq \frac{2C^2}{V^4} \frac{p_\perp dp_\perp x dx}{(2\pi)^2 2(1-x)} \times \left[p_\perp^2 |\mathcal{A}_+^{(0,0)}|^2 + p_\perp^2 |\mathcal{A}_-^{(0,0)}|^2 + \dots \right] \\ &\quad \times \frac{1}{2E_q 2E_W |v_W - v_X|} d\Phi_Y (2\pi)^4 \delta^4(p_Y - p_W - p_X) \end{aligned}$$

What if it is subject to the 'helicity selection rule'

$$\boxed{\mathcal{A}_{-,SM}^{(0,0)} \neq 0}$$

$$\mathcal{A}_{-,BSM}^{(0,0)} = 0$$

$$e^{-2i\phi} \mathcal{A}_{-,SM}^{(0,0)*} \mathcal{A}_{+,BSM}^{(0,0)} + h.c.$$

$$\boxed{\mathcal{A}_{+,SM}^{(0,0)} = 0}$$

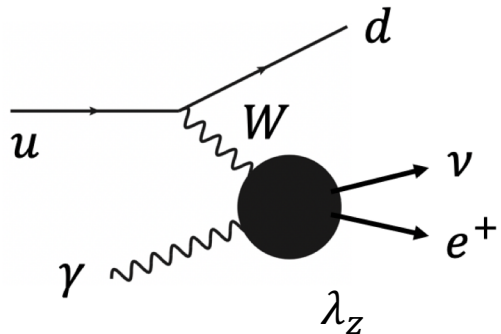
$$\boxed{\mathcal{A}_{+,BSM}^{(0,0)} \neq 0}$$

vanishes upon the integration over ϕ

: it meets our usual expectation, or EWA

Beyond the relevant region for EWA

Including only transverse polarization ...



$$\begin{aligned} \mathcal{A}_{\text{total}} = & \frac{2C}{V^2} \left[\tilde{p}_\perp \left(\mathcal{A}_+^{(0,0)} + \mathcal{A}_+^{(1,0)} \frac{\tilde{p}_\perp}{E} + \mathcal{A}_+^{(0,1)} \frac{\tilde{p}_\perp^*}{E} + \dots \right) \right. \\ & \left. + \tilde{p}_\perp^* \left(\mathcal{A}_-^{(0,0)} + \mathcal{A}_-^{(1,0)} \frac{\tilde{p}_\perp}{E} + \mathcal{A}_-^{(0,1)} \frac{\tilde{p}_\perp^*}{E} + \dots \right) \right] \\ \tilde{p}_\perp \equiv & p_1 - ip_2 = p_\perp e^{-i\phi}, \tilde{p}_\perp^* = p_\perp e^{i\phi} \end{aligned}$$

From our computation for the left-handed photon

$$\boxed{\mathcal{A}_{-,SM}^{(0,0)} \neq 0}$$

$$\mathcal{A}_{-,BSM}^{(0,0)} = 0$$

$$\mathcal{A}_{+,SM}^{(0,0)} = 0$$

$$\boxed{\mathcal{A}_{+,BSM}^{(0,0)} \neq 0}$$

Leading ϕ – independent contributions

: interference will not be caught in EWA

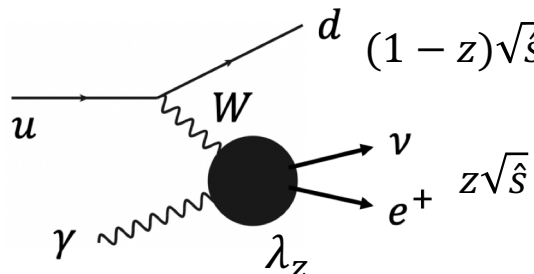
$$\left(\frac{\tilde{p}_\perp \tilde{p}_\perp^*}{E^2} \right)^2 \left(\mathcal{A}_{-,SM}^{(1,0)*} \mathcal{A}_{+,BSM}^{(0,1)} + h.c. \right)$$

$$\left(\frac{\tilde{p}_\perp \tilde{p}_\perp^*}{E^2} \right) \left| \mathcal{A}_{-,SM}^{(0,0)} \right|^2 + \left(\frac{\tilde{p}_\perp \tilde{p}_\perp^*}{E^2} \right) \left| \mathcal{A}_{+,BSM}^{(0,0)} \right|^2$$

$$\frac{|\mathcal{A}|_{SM \times BSM}^2}{|\mathcal{A}|_{SM}^2} \propto \lambda_z \left(\frac{\tilde{p}_\perp}{E} \right)^2 \frac{E^2}{m^2}$$

$$\frac{|\mathcal{A}|_{BSM^2}^2}{|\mathcal{A}|_{SM}^2} \propto \lambda_z^2 \frac{E^4}{m^2}$$

Beyond the relevant region for EWA



$$p_T(q) = (1 - z)\sqrt{\hat{s}} \sin \theta$$

$$m_{e\nu} = (2z - 1)\sqrt{\hat{s}} = E$$

$$p_T(q) = p_\perp \sim E\theta \quad \text{for } \theta \ll 1, z \sim \mathcal{O}(1) \rightarrow \theta \sim \frac{p_\perp}{E}$$

$$\epsilon_L \cdot \mathcal{M} = \sum_m C_m e^{\pm im\phi}$$

in the unitary gauge

$$\begin{aligned} \epsilon_L \cdot \mathcal{M}_{BSM} &= \lambda_z \frac{eg^2}{4m_W^2} \frac{\hat{s}^{5/2} \sqrt{(2z-1)(1-z)} \sin \frac{\theta}{2} e^{-i\phi}}{[(2z-1)\hat{s} - m_W^2] [m_W^2 + \hat{s}(1-z)(1-\cos\theta)]} \\ &\times \left[2\sqrt{2z-1} \sin \psi \cos \theta - (1 - \cos \psi) \sin \theta e^{-i\phi} \right. \\ &\quad \left. + (2z-1)(1 + \cos \psi) \sin \theta e^{i\phi} \right], \end{aligned}$$

$$\begin{aligned} \epsilon_L \cdot \mathcal{M}_{SM} &= -eg^2 \frac{1}{m_W^2 + \hat{s}(1-z)(1-\cos\theta)} \left[\hat{s}^{3/2} \sqrt{\frac{1-z}{2z-1}} (1 + \cos \psi) \sec \frac{\theta}{2} \right. \\ &\times \frac{4(1-z)(2z-1)(1-\cos\theta) - 2(5-4z) \frac{m_W^2}{\hat{s}}}{6 [(2z-1)\hat{s} - m_W^2]} \\ &+ \hat{s}^{1/2} \frac{(1-z)^{3/2}}{2z-1} \sin \psi \sec^3 \frac{\theta}{2} \sin \theta e^{i\phi} \\ &+ \hat{s}^{1/2} \left(\frac{1-z}{2z-1} \right)^{3/2} \frac{1}{2} (1 - \cos \psi) \sec^5 \frac{\theta}{2} \sin^2 \theta e^{2i\phi} \\ &\quad \left. + \hat{s}^{1/2} \frac{(1-z)^{3/2}}{(2z-1)^2} \frac{1}{4} (1 - \cos \psi)^2 \csc \psi \sec^7 \frac{\theta}{2} \sin^3 \theta e^{3i\phi} + \dots \right], \end{aligned}$$

for $\theta \ll 1$

$$\epsilon_L \cdot \mathcal{M} = \tilde{\theta} \left(\mathcal{M}_+^{(0,0)} + \mathcal{M}_+^{(1,0)} \tilde{\theta} + \mathcal{M}_+^{(0,1)} \tilde{\theta}^* + \dots \right)$$

$$+ \tilde{\theta}^* \left(\mathcal{M}_-^{(0,0)} + \mathcal{M}_-^{(1,0)} \tilde{\theta} + \mathcal{M}_-^{(0,1)} \tilde{\theta}^* + \dots \right)$$

$$\tilde{\theta} \equiv \theta e^{-i\phi}$$

In this limit, it can be compared with Borel et al.

However, our result work for sizable angle which captures the beyond the EWA phase space

2-to-4 dilepton + 2 jets

Numerical Result



CERN-EP-2017-328
2018/07/24

CMS-SMP-16-018

Electroweak production of two jets in association with a Z boson in proton-proton collisions at $\sqrt{s} = 13 \text{ TeV}$

Our validation

CMS-SMP-16-018

Sample	Initial	
	ee	$\mu\mu$
$t\bar{t}$	5454 (5363 \pm 48)	13962 (12938 \pm 81)
DY Zjj (pythia8)	146147 (152750 \pm 510)	373731 (394640 \pm 880)
EW Zjj (pythia8)	2639 (2833 \pm 10)	6328 (6665 \pm 16)

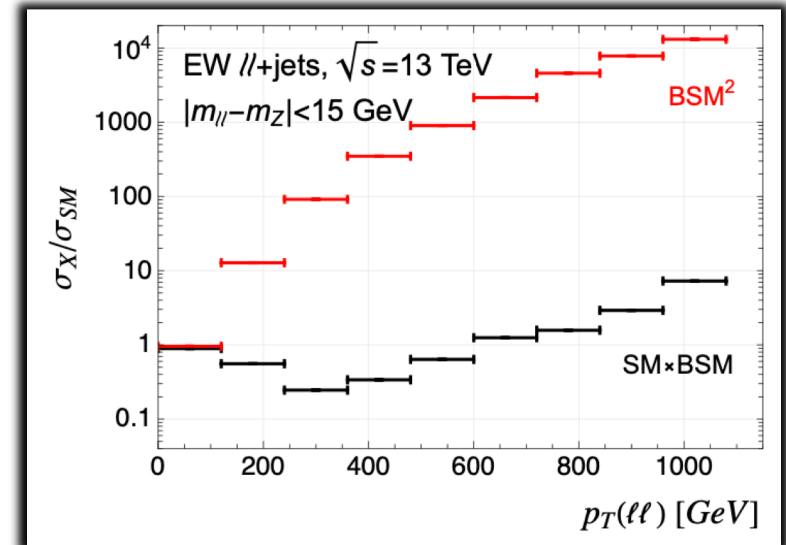
↑
Initial cuts

$$p_T(\ell_1) > 30 \text{ GeV}, \quad p_T(\ell_2) > 20 \text{ GeV}, \quad |\eta(\mu)| < 2.4, \quad |\eta(e)| < 2.1$$

$$p_T(j_1) > 50 \text{ GeV}, \quad p_T(j_2) > 30 \text{ GeV}, \quad |\eta(j)| \leq 4.7,$$

$$|m_Z - m_{\ell\ell}| < 15 \text{ GeV}, \quad m_{jj} > 200 \text{ GeV}.$$

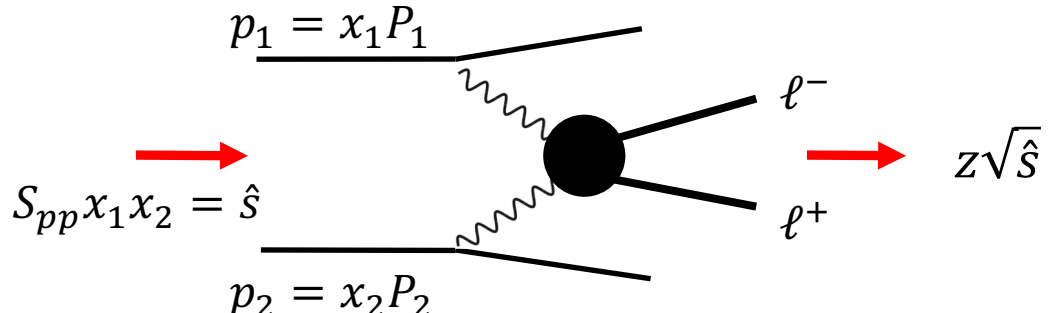
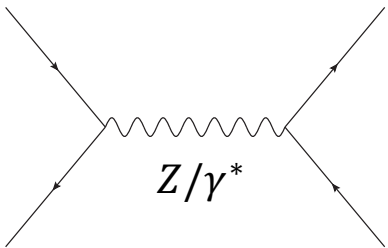
* Note CMS analysis consider only events in Z mass window



Interference can be accessed through

$$\frac{d\sigma/d\phi}{d\sigma_{SM}/d\phi}$$

Control Hardness of the process



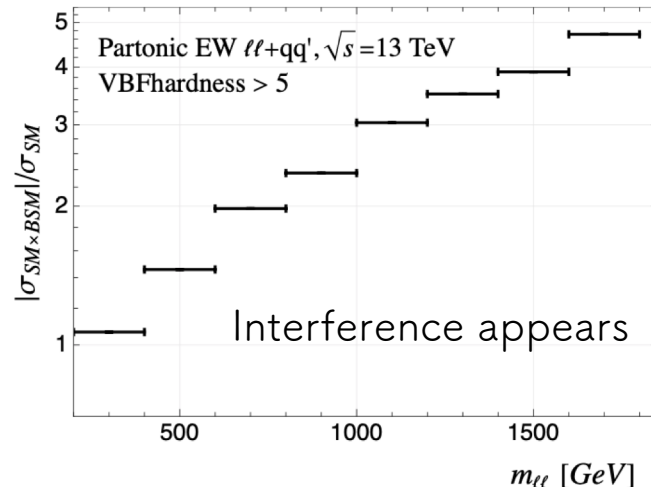
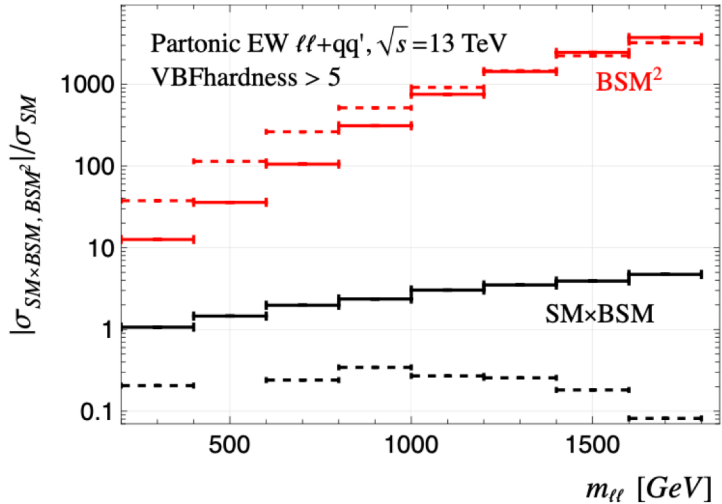
$$m_{\ell\ell}^2 = \hat{s} = x_1 x_2 S_{pp}$$

$$m_{\ell\ell}^2 - m_{qq'}^2 = (2z - 1)\hat{s}$$

QCD Drell-Yan

EW Drell-Yan

$$VBFhardness = \frac{m_{\ell\ell}^2 - m_{qq'}^2}{p_T^2(qq') \cosh^2 \eta_{qq'} + m_{qq'}^2} = \frac{2z - 1}{(1 - z)^2} \quad : \text{monotonically increasing function}$$



Summary

EW dilepton process can access a wider phase space beyond the EWA limit and resurrect the interference in the total cross section, as opposed to the differential cross section

Soft-phase space enhanced interference (t-channel)

Our toy process provides an explicit analytic understanding of the above feature

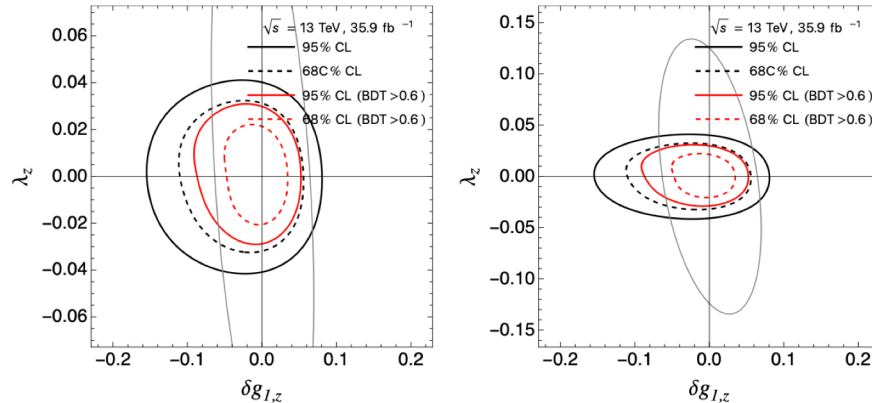
We proposed a new variable controlling the hardness of the subprocess, namely VBFhardness

Might be useful for any VBF-process

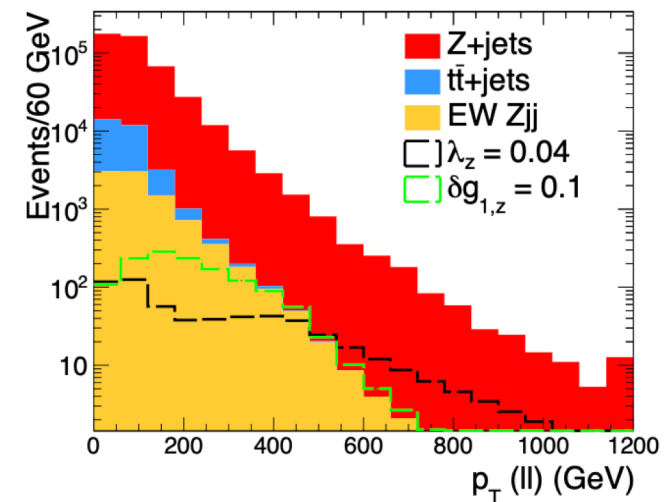
On the sensitivity of aTGC

In Z mass window

$$\begin{aligned} p_T(\ell_1) &> 30 \text{ GeV}, & p_T(\ell_2) &> 20 \text{ GeV}, & |\eta(\mu)| &< 2.4, & |\eta(e)| &< 2.1 \\ p_T(j_1) &> 50 \text{ GeV}, & p_T(j_2) &> 30 \text{ GeV}, & |\eta(j)| &\leq 4.7, \\ |m_Z - m_{\ell\ell}| &< 15 \text{ GeV}, & m_{jj} &> 200 \text{ GeV}. \end{aligned}$$

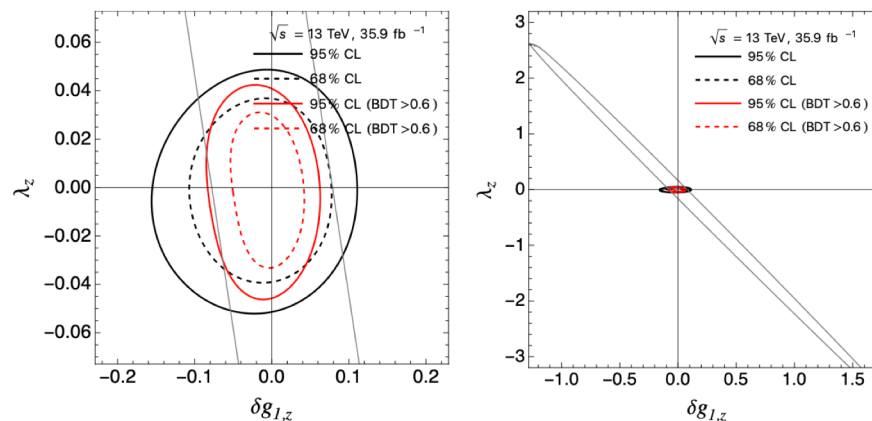


35.9 fb⁻¹ (13 TeV)

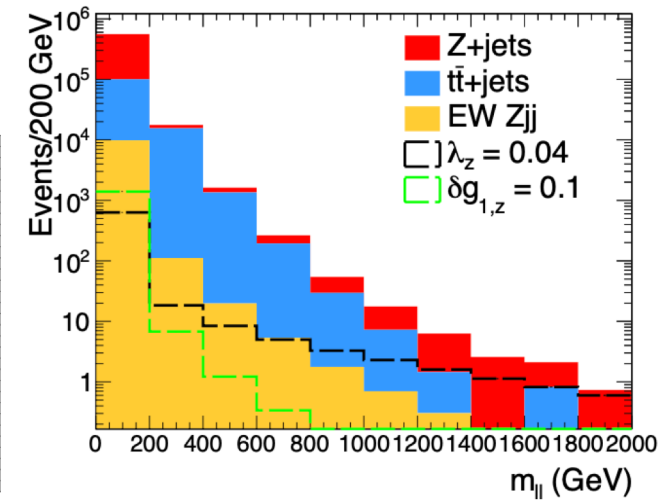


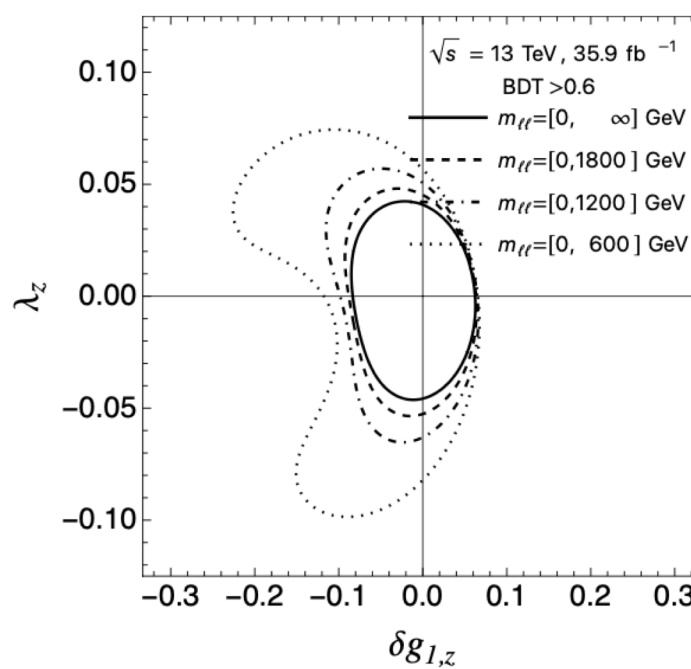
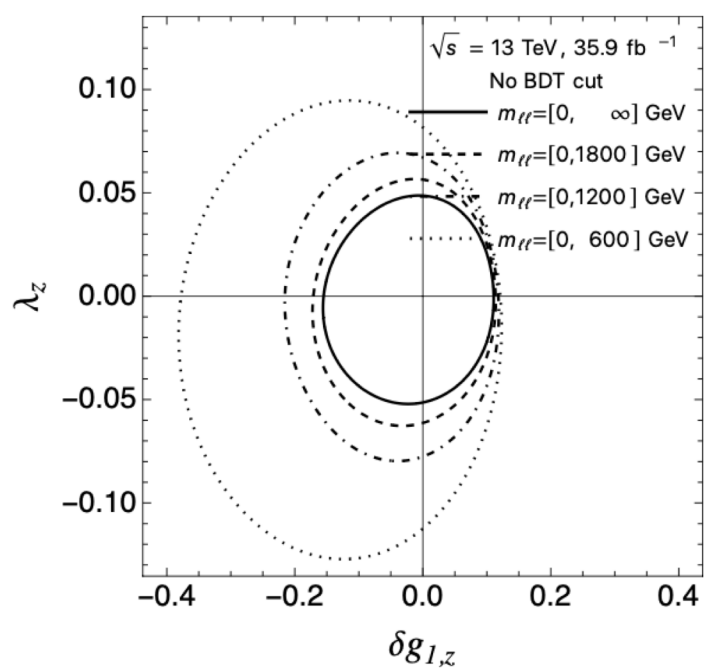
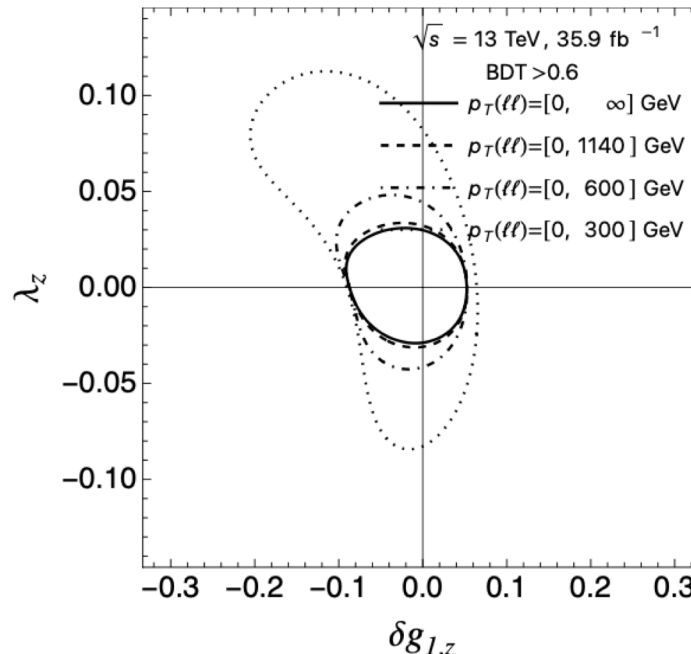
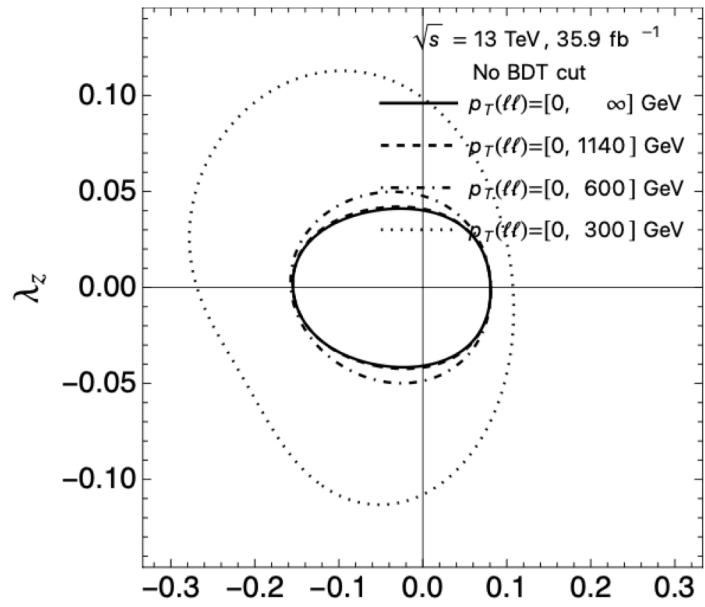
Off-shell region away from Z mass window

$$\begin{aligned} p_T(\ell_1) &> 30 \text{ GeV}, & p_T(\ell_2) &> 20 \text{ GeV}, & |\eta(\mu)| &< 2.4, & |\eta(e)| &< 2.1 \\ p_T(j_1) &> 50 \text{ GeV}, & p_T(j_2) &> 30 \text{ GeV}, & |\eta(j)| &\leq 4.7, \\ m_{jj} &> 200 \text{ GeV}. \end{aligned}$$



35.9 fb⁻¹ (13 TeV)





Practical relevance of EW dilepton process ?

Di-boson

CMS $W\gamma$

$L = 138 \text{ fb}^{-1}$



CMS-SMP-20-005

CERN-EP-2021-219
2022/03/11

Measurement of $W^\pm\gamma$ differential cross sections in proton-proton collisions at $\sqrt{s} = 13 \text{ TeV}$ and effective field theory constraints

Table 4: Best fit values of C_{3W} and corresponding 95% CL confidence intervals as a function of the maximum p_T^γ bin included in the fit.

p_T^γ cutoff (GeV)	Best fit C_{3W} (TeV^{-2}) SM+int. only	Best fit C_{3W} (TeV^{-2}) SM+int.+BSM	Observed 95% CL (TeV^{-2}) SM+int. only	Observed 95% CL (TeV^{-2}) SM+int.+BSM	Expected 95% CL (TeV^{-2}) SM+int. only	Expected 95% CL (TeV^{-2}) SM+int.+BSM
200	-0.86	-0.24	[-2.01, 0.38]	[-0.76, 0.40]	[-1.16, 1.27]	[-0.81, 0.71]
300	-0.25	-0.17	[-0.81, 0.34]	[-0.39, 0.28]	[-0.56, 0.60]	[-0.33, 0.33]
500	-0.13	-0.025	[-0.50, 0.25]	[-0.15, 0.12]	[-0.35, 0.38]	[-0.17, 0.16]
800	-0.20	-0.033	[-0.49, 0.11]	[-0.10, 0.08]	[-0.29, 0.31]	[-0.097, 0.095]
1500	-0.13	-0.009	[-0.38, 0.17]	[-0.062, 0.052]	[-0.27, 0.29]	[-0.066, 0.065]

$$C_{3W}\epsilon_{ijk}W_{\mu\nu}^iW_{\nu\rho}^jW_{\rho\mu}^k \quad \text{In Warsaw basis}$$

$$C_{3W} = [-0.062, 0.052] @ 95\% \text{CL}$$

VBF EW dilepton

CMS $Z(\ell\ell) + 2j \quad L = 35.9 \text{ fb}^{-1}$



CMS-SMP-16-018

CERN-EP-2017-328
2018/07/24

Electroweak production of two jets in association with a Z boson in proton-proton collisions at $\sqrt{s} = 13 \text{ TeV}$

Coupling constant	Expected 95% CL interval (TeV^{-2})	Observed 95% CL interval (TeV^{-2})
c_{WWW}/Λ^2	[-3.7, 3.6]	[-2.6, 2.6]

$$\frac{c_{WWW}}{\Lambda^2} \text{Tr}(\hat{W}_{\mu\nu} \hat{W}_{\nu\rho} \hat{W}_{\rho\mu}) \quad \text{Hagiwara et. al. (HISZ basis), Degrande et. al.}$$

$$= \frac{c_{WWW}g^3}{4\Lambda^2} \epsilon_{ijk} W_{\mu\nu}^i W_{\nu\rho}^j W_{\rho\mu}^k \quad \rightarrow \quad C_{3W} = \frac{c_{WWW}g^3}{\Lambda^2} \frac{1}{4}$$

$$C_{3W}^{\text{assuming } 138 \text{ fb}^{-1}} \sim [-2.6, 2.6] \times 0.07 \times \frac{1}{\sqrt{1.97}} = [-0.13, 0.13]$$

Our recasting is 3 x weaker than CMS VBF EW dilepton. Remains to be settled down.